(12)

AD

AD A113210

TECHNICAL REPORT ARLCB-TR-82004

THERMAL RELAXATION IN AUTOFRETTAGED CYLINDERS

Joseph F. Throop
John H. Underwood
Gregory S. Leger

March 1982

US ARMY ARMAMENT RESEARCH AND DEVELOPMENT COMMAND
LARGE CALIBER WEAPON SYSTEMS LABORATORY
BENÉT WEAPONS LABORATORY
WATERVLIET, N. Y. 12189

AMCMS No. 6121.05.HB40.0

PRON No. AW-1-RBWL1-AW1A

APPROVED FOR PUBLIC RELEASE; DISTRIBUTION UNLIMITED

DISCLAIMER

The findings in this report are not to be construed as an official Department of the Army position unless so designated by other authorized documents.

The use of trade name(s) and/or manufacture(s) does not constitute an official indorsement or approval.

DISPOSITION

Destroy this report when it is no longer needed. Do not return it to the originator.

SECURITY CLASSIFICATION OF THIS PAGE (When Data Entered)

REPORT DOCUMENTATION PAGE

READ INSTRUCTIONS BEFORE COMPLETING FORM

1. REPORT NUMBER: ARLCB-TR-82004	2. GOVT ACCESSION NO.: AD-A113 2??
3. RECIPIENT'S CATALOG NUMBER	
4. TITLE (and Subtitle): THERMAL RELAXATION IN AUTOFRETTAGED CYLINDERS	5. TYPE OF REPORT & PERIOD COVERED: Final
	6. PERFORMING ORG. REPORT NUMBER
7. AUTHOR(s): Joseph F. Throop, John H. Underwood, and Gregory S. Leger	8. CONTRACT OR GRANT NUMBER(s)
9. PERFORMING ORGANIZATION NAME AND ADDRESS: US Army Armament Research & Development Command, Benet Weapons Laboratory, DRDAR-LCB-TL, Watervliet, NY 12189	10. PROGRAM ELEMENT, PROJECT, TASK AREA & WORK UNIT NUMBERS: AMCMS No. 6121.05.HB40.0, PRON No. AW-1-RBWL1-AW1A
11. CONTROLLING OFFICE NAME AND ADDRESS: US Army Armament Research & Development Command, Large Caliber Weapon Systems Laboratory, Dover, NJ 07801	12. REPORT DATE: March 1982
	13. NUMBER OF PAGES: 38
14. MONITORING AGENCY NAME & ADDRESS (if different from Controlling Office)	15. SECURITY CLASS. (of this report): UNCLASSIFIED
	15a. DECLASSIFICATION/DOWNGRADING SCHEDULE

16. DISTRIBUTION STATEMENT (of this Report)

Approved for public release; distribution unlimited.

17. DISTRIBUTION STATEMENT (of the abstract entered in Block 20, if different from Report)

18. SUPPLEMENTARY NOTES

Presented at 28th Sagamore Army Materials Research Conference, Lake Placid, NY, 13-17 July 1981.
Published in proceedings of the conference.

19. KEY WORDS (Continue on reverse side if necessary and identify by block number)

Autofrettaged Cylinders
Overstrain
Residual Stresses
Thermal Gradient
Thermal Stresses
Relaxation
Bore Closure

20. ABSTRACT (Continue on reverse side if necessary and identify by block number)

This report presents an experimental study on the loss of bore expansion and change of residual stresses in autofrettaged cylinders, resulting from internal heating combined with external cooling. It provides information useful in the design of pressure vessels operating at high temperature. Two-foot long cylinders were heated internally to bore temperatures up to 950°F and simultaneously cooled externally to produce a temperature difference of as

(CONT'D ON REVERSE)

DD FORM 1 JAN 73 1473 EDITION OF 1 NOV 65 IS OBSOLETE

UNCLASSIFIED

SECURITY CLASSIFICATION OF THIS PAGE (When Data Entered)

20. ABSTRACT (CONT'D)

much as 725°F from bore to outside surface. Reduction of the autofrettage bore expansion and reduction of residual stresses resulted, because the thermal stresses added to the residual stresses and exceeded the lowered yield strength at elevated temperature, permitting relaxation to occur.

The data reveals that under certain temperature conditions a considerable portion of the autofrettage induced bore expansion and the associated residual stresses can be lost in a few minutes when external cooling occurs. The experimental results indicate that partial overstrain in autofrettage may be preferable to full overstrain in order to minimize the loss in residual stress.

TABLE OF CONTENTS

TABLES

LIST OF ILLUSTRATIONS

ACKNOWLEDGEMENT

This work was performed under funding from Project Number 612105.H840011 of the Army Materials and Mechanics Research Center, Watertown, MA. We are pleased to acknowledge the help of R. R. Fujczak, R. T. Abbott, W. M. Yaiser, H. R. Alford, and C. C. DeLaMater in performing the experiments described here, of C. Prokrym for photography and of Ellen Fogarty for preparing the manuscript.

LIST OF SYMBOLS AND TERMS

a - radius to inside wall

b - radius to outside wall

r - radius to any point in the wall

ρ - radius of the elastic-plastic interface

OD - outside diameter of ring

ID - inside diameter of ring

γ - angle of opening of the ring at the slit

M - moment needed to close slit opening of the ring

σ_θ - tangential stress

σ_y - yield strength

$\Delta\varepsilon_\theta$ - change in tangential strain

BC - bore closure; loss of bore expansion

BE - bore enlargement

E - modulus of elasticity = 30×10^6 psi

Separation Angle Ratio - $\dfrac{\gamma_{experimental}}{\left(\dfrac{3\pi}{\sqrt{3}E}\sigma_y\right)}$

Residual Stress Ratio - $\dfrac{\sigma_{\theta experimental}}{\sigma_{\theta theoretical}}$

Bore Enlargement Ratio - $\dfrac{BE_{final}}{BE_{initial}}$

INTRODUCTION

In any prestressed structure the loss of prestress in service can result in improper functioning or in failure. In pressure vessels the loss of autofrettage-induced residual stresses can result in permanent contraction of the bore and in reduction of the improvement in fatigue life provided by the compressive residual bore stress. Relaxation may be brought about by yielding at the elevated bore temperature as the result of a thermal stress gradient caused by internal heating and external cooling. Although relaxation cannot be totally prevented, it can be controlled by limiting the autofrettage overstrain to suit the severity of the thermal gradient.

A 1969 paper by Dawson and Jackson[1] studied the relaxation of residual stresses in autofrettaged cylinders subjected to oven heating in a salt bath up to 850°F for as long as 72 hours. They found "that for a given temperature and time the bore tangential stress relaxes in a manner that can be predicted by means of creep data." They concluded that "the autofrettage process could be used to significantly extend the creep life of an autoclave provided that there is proper control of pressure and temperature," and "that the design of autofrettaged autoclaves is amenable to an analytical approach." Their study, however, did not include a temperature gradient in the cylinders.

---

[1]Dawson, V. C. D. and Jackson, J. W., "Investigation of the Relaxation of Residual Stresses in Autofrettaged Cylinders," Trans. of ASME, Jour. of Basic Engineering, Vol. 91, Series D, No. 1, pp. 63-66, March 1969.

OBJECT

The present experimental study was initiated to determine the amount of overstrain permissible without causing excessive bore closure due to temperature effects in pressure vessels. Our purpose was to measure the amount of permanent bore contraction resulting from the combination of lowered yield strength, thermal stress gradient, and residual stress gradient at a variety of bore temperatures and temperature distributions. Work has been continued toward finding ways to evaluate the changes in residual stresses as functions of the bore temperature, the temperature gradient, and the starting amount of autofrettage overstrain. Recently, analytical approaches have become available, involving relations between thermal and residual stress distributions, superposition techniques, and finite element analysis, which can provide solutions for these problems.

The following experimental results and data analysis are informative in themselves as to the nature and magnitude of the relaxation phenomena when it occurs in large pressure vessels. They are offered, as well, as material with which to test and verify such analytical formulations. One important application is in the evaluation of stress intensity factors for cracks in the residual stress fields of autofrettaged thick walled cylinders for calculation of fatigue lives.

SPECIMENS

The bore closure studies were conducted using smooth-bore cylinders 25 inches long. These cylinders were machined with several bore sizes and outer diameters so that autofrettage with a given size mandrel would produce three pairs of cylinders with a diameter ratio, OD/ID of 2.14 and three pairs with OD/ID of 1.82. For each size, one pair had 100%, one pair had 75%, and one pair had 50% overstrain. The dimensions and permanent bore expansions are listed in Table I. A one-inch ring was cut off the end of each cylinder prior to the heating experiment to be used for initial residual stress measurements.

TABLE I. DIMENSIONS AND AUTOFRETTAGE BORE EXPANSIONS

OD/ID = 2.14	OD/ID = 1.82
100% Overstrain ID = 4.022" OD = 8.695" Bore Expansion = 0.0510" Yield Strength = 166 Ksi	100% Overstrain ID = 4.042" OD = 7.405" Bore Expansion = 0.0300" Yield Strength = 174 Ksi
75% Overstrain ID = 4.042" OD = 8.735" Bore Expansion = 0.0330" Yield Strength = 170 Ksi	75% Overstrain ID = 4.060" OD = 7.435" Bore Expansion = 0.0200" Yield Strength = 168 Ksi
50% Overstrain ID = 4.060" OD = 8.775" Bore Expansion = 0.0170" Yield Strength = 169 Ksi	50% Overstrain ID = 4.071" OD = 7.455" Bore Expansion = 0.0100" Yield Strength = 164 Ksi

PROCEDURE

For the purpose of heating, a large blowtorch was utilized as shown in Figure 1. A stainless steel cone was bolted to the specimen for concentrating the flame into the bore. This procedure produced nominal bore temperatures (Ta) of 950°F at the hot end station, 730°F at the mid-length, and 650°F at the exit end station. Cooling was accomplished by means of an externally mounted perforated coil.

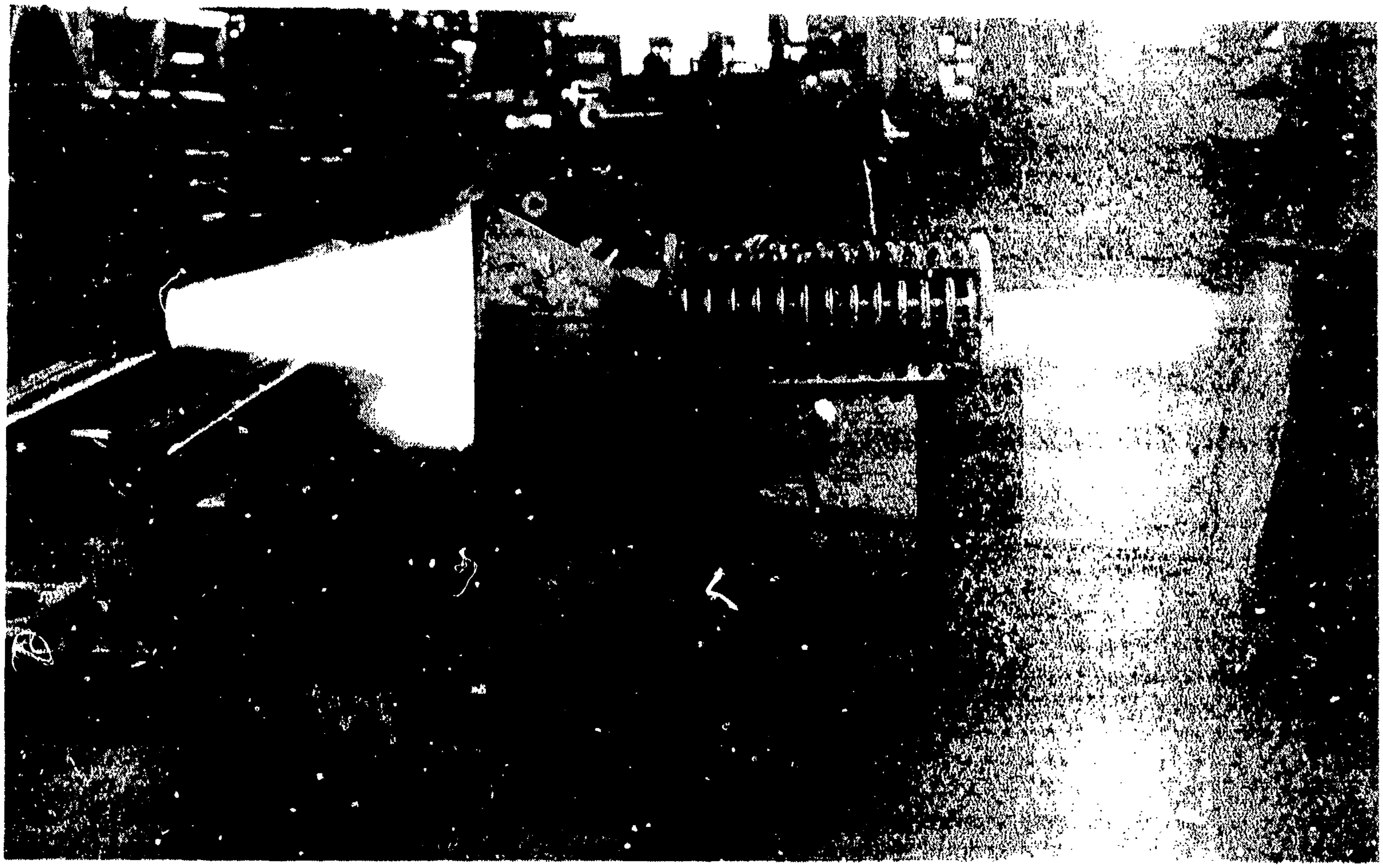

Figure 1. Heating and Cooling Arrangement

The outside surface was cooled by either convection or using a coil for air-water mist or a water spray. Four test conditions were used, giving four ranges of temperature difference, ΔT, between the ID and OD: (1) up to 100°F with natural convection cooling, (2) from 100°F to 300°F with forced air cooling, (3) from 300°F to 450°F with air-water mist and (4) from 450°F to 800°F with water spray cooling. The conditions were maintained for 15 minutes.

Temperature measurement was obtained during the heating-quenching operation by means of continuously measured chromel-alumel thermocouples, welded to the OD surface and at two depths in the cylinder wall, mid-thickness and 1/4 inch from the bore surface.

One inch thick rings were cut from the three stations for residual stress measurement; these rings being located at 5, 12.5, and 20 inches from the hot end of the specimen. Residual stress measurement was performed by slitting of the rings and measuring punch mark separation, by SR-4 strain gages mounted adjacent to the slit, and by measurement of angle of slit opening. The strain gage approach is felt to give the most accurate measurement of stress relief at the cylinder surfaces.

While the angle of opening can be measured repeatedly to insure accuracy, the stress relieved is calculated from the angle by substitution into equations relating the stress to the moment required to close the gap in a curved beam. This permits calculation of stress values for any desired radii, but does not give the actual stress relieved at a particular point in the cylinder wall.

For purpose of comparison, several rings from autofrettaged, non-heated cylinders were exposed to steady state uniform furnace heating.

RESULTS AND DISCUSSION

The strains relieved and the separation angles measured are listed in Table II. In this table the bore enlargement, ΔD, is the difference between the original bore diameter prior to autofrettage and the final diameter subsequent to the autofrettage and thermal treatment listed in Table II. Percent overstrain is defined as $\%OS = 100(\rho-a)/(b-a)$ where ρ is the elastic-plastic interface radius and b and a the external and internal radius respectively.

The relaxed residual stress measured after thermal exposure is compared with the theoretical residual stress calculated using the distortion energy theory yield criterion of von Mises. The equations[2] for tangential residual stress σ_θ and radial residual stress σ_r are:

$$\sigma_\theta = \begin{cases} \dfrac{2\sigma_y}{\sqrt{3}} \left\{ \dfrac{a^2}{b^2-a^2} \left[1 + \dfrac{b^2}{r^2}\right] \left[\dfrac{\rho^2-b^2}{2b^2} - \ln \dfrac{\rho}{a}\right] + \left[\dfrac{\rho^2+b^2}{2b^2} - \ln \dfrac{\rho}{r}\right] \right\} & a<r<\rho \\[2ex] \dfrac{2\sigma_y}{\sqrt{3}} \left[1 + \dfrac{b^2}{r^2}\right] \left\{ \dfrac{\rho^2}{2b^2} + \dfrac{a^2}{b^2-a^2} \left[\dfrac{\rho^2-b^2}{2b^2} - \ln \dfrac{\rho}{a}\right] \right\} & \rho<r<b \end{cases} \qquad (1)$$

$$\sigma_r = \begin{cases} \dfrac{2\sigma_y}{\sqrt{3}} \left\{ \left[\dfrac{a^2}{b^2-a^2}\right] \left[1 - \dfrac{b^2}{r^2}\right] \left[\dfrac{\rho^2-b^2}{2b^2} - \ln \dfrac{\rho}{a}\right] + \left[\dfrac{\rho^2-b^2}{2b^2} - \ln \dfrac{\rho}{r}\right] \right\} & a<r<\rho \\[2ex] \dfrac{2\sigma_y}{\sqrt{3}} \left[1 - \dfrac{b^2}{r^2}\right] \left\{ \dfrac{\rho^2}{2b^2} + \dfrac{a^2}{b^2-a^2} \left[\dfrac{\rho^2-b^2}{2b^2} - \ln \dfrac{\rho}{a}\right] \right\} & \rho<r<b \end{cases} \qquad (2)$$

where σ_y is the yield strength, a is the inside radius, b is the outside radius and ρ is the radius to the elastic-plastic interface.

---

[2]Davidson, T. E., Barton, C. S., Reiner, A. N., and Kendall, D. P., "Overstrain of High Strength, Open End Cylinders of Intermediate Diameter Ratio," Proc. 1st International Congress on Experimental Mechanics, pp. 335-352, Pergamon Press, Oxford, 1963.

TABLE IIa. STRAINS RELIEVED AND SEPARATION ANGLES

OD/ID = 2.14					
Type	Bore Enlargement (in.)	Strains Relieved $\Delta\varepsilon$ (μ in/in)		Separation Angle (deg.)	Punch Mark Separation (in.)
100% OS	ΔD	ID	OD	γ	OD
Unfired	0.0510	+4213	-1927	3.90	0.325
Ta = 648°F ΔT = 422	0.0464	-	-	-	-
Ta = 736 ΔT = 541	0.0451	+3477	-1920	-	0.245
Ta = 932 ΔT = 673	0.0362	+2288	-20	1.85	0.130
75% OS					
Unfired	0.0330	+4953	-1147	3.63	0.280
Ta = 685°F ΔT = 490	0.0295	-	-	-	-
Ta = 760 ΔT = 516	0.0289	+4152	-1156	3.30	0.230
Ta = 947 ΔT = 726	0.0176	+2700	-654	2.08	0.160
50% OS					
Unfired	0.0170	+4357	-1104	2.96	0.200
Ta = 638°F ΔT = 418	0.0143	-	-	-	-
Ta = 733 ΔT = 456	0.0142	+3295	-1387	2.66	0.175
Ta = 969 ΔT = 740	0.0079	+144	-145	1.56	0.095

TABLE IIb. STRAINS RELIEVED AND SEPARATION ANGLES

OD/ID = 1.82					
Type	Bore Enlargement (in.)	Strains Relieved Δε (μ in/in)		Separation Angle (deg.)	Punch Mark Separation (in.)
100% OS	ΔD	ID	OD	Y	OD
Unfired	0.0300	+4870	-	5.25	0.315
Ta = 656°F ΔT = -	0.0287	+4195	-3272	4.87	0.295
Ta = 793 ΔT = 574	0.0288	+3090	-2805	4.59	0.270
Ta = 1123 ΔT = 802	0.0239	+957	-1441	2.20	0.295
75% OS					
Unfired	0.0200	+4065	-2445	4.42	0.260
Ta = 641°F ΔT = 409	0.0198	+3745	-2325	4.37	0.250
Ta = 798 ΔT = 532	0.0190	+3117	-1698	3.85	0.245
Ta = 956 ΔT = 726	0.0149	+861	-1552	2.80	0.160
50% OS					
Unfired	0.0100	+1523	-1708	3.60	0.170
Ta = 650°F ΔT = 466	0.0098	+2903	-1045	3.38	0.175
Ta = 745 ΔT = 452	0.0090	+2818	-1552	-	0.165
Ta = 939 ΔT = 722	0.0070	+1567	-887	2.00	0.110

The tangential residual stress σ_θ is of main interest because of the beneficial effects of compressive residual stress σ_θ at the bore, which results in enhanced resistance to yielding and to fatigue.

Calculation of the stress relieved by slitting the rings, using strain gage measurements, employed the uniaxial stress-strain relationship

$$\sigma_\theta = E(\Delta\varepsilon_\theta)$$

where E is 30×10^6 psi and $\Delta\varepsilon_\theta$ is the change in strain measured with a tangential strain gage in microinch per inch.

From the angle γ of opening of the ring at the slit the residual stress is calculated by means of the moment M required to close the gap to form a closed ring. The ring is assumed to act elastically as a curved beam and to require a pure bending moment on the slit surface.[3] This moment is given by

$$M = \frac{\gamma E}{8\pi}\left[\frac{(b^2-a^2)^2 - 4a^2b^2(\ln(b/a))^2}{2(b^2-a^2)}\right] \quad (3)$$

The stress at any radius r is then calculated from

$$\sigma_\theta = \frac{-4M}{N}\left[\frac{-a^2b^2}{r^2}\ln(b/a) + b^2\ln(r/b) + a^2\ln(a/r) + b^2-a^2\right] \quad (4)$$

$$\sigma_r = \frac{-4M}{N}\left[\frac{-a^2b^2}{r^2}\ln(b/a) + b^2\ln(r/b) + a^2\ln(a/r)\right] \quad (5)$$

where $N = (b^2-a^2) - 4a^2b^2(\ln(b/a))^2$

a is the radius to the inside surface and

b is the radius to the outside surface.

---

[3]Timoshenko, S. and Goodier, J. N., "Theory of Elasticity," Second Edition, McGraw Hill, NY (1951), pp. 60-69, Third Edition, McGraw HIll, NY (1970), pp. 68-80.

Equations (4) and (5) do not apply for cases other than 100% overstrain, hence further analysis is necessary to evaluate the stresses in partially overstrained cylinders.

The following graphs show the expected and measured residual stresses, bore closure and their variation with thermal gradient test conditions in cylinders of two diameter ratios, 2.14 and 1.82.

Figures 2 and 3 respectively show the theoretical distribution of residual stress for 2.14 and 1.82 diameter ratio, for percent overstrains of 25%, 50%, 75%, and 100%.

Figure 4 shows the temperature distribution through the thickness of the cylinder wall. The data points are for forced air cooling of the 2.14 diameter ratio cylinder. The curves are plots of the theoretical logarithmic steady-state temperature distribution[4] calculated for the temperature difference ΔT which was measured between the ID and OD with imbedded thermocouples. The good agreement between data points and theory indicates that the test conditions were close to the steady-state. This thermal condition produces an associated stress distribution of the same shape as that for 100% overstrain, with compression at the bore and tension at the OD that increase with increasing ΔT.

[4]Kreith, F., "Principles of Heat Transfer," International Textbook Co., Scranton, PA, 1958, pp. 25-29.

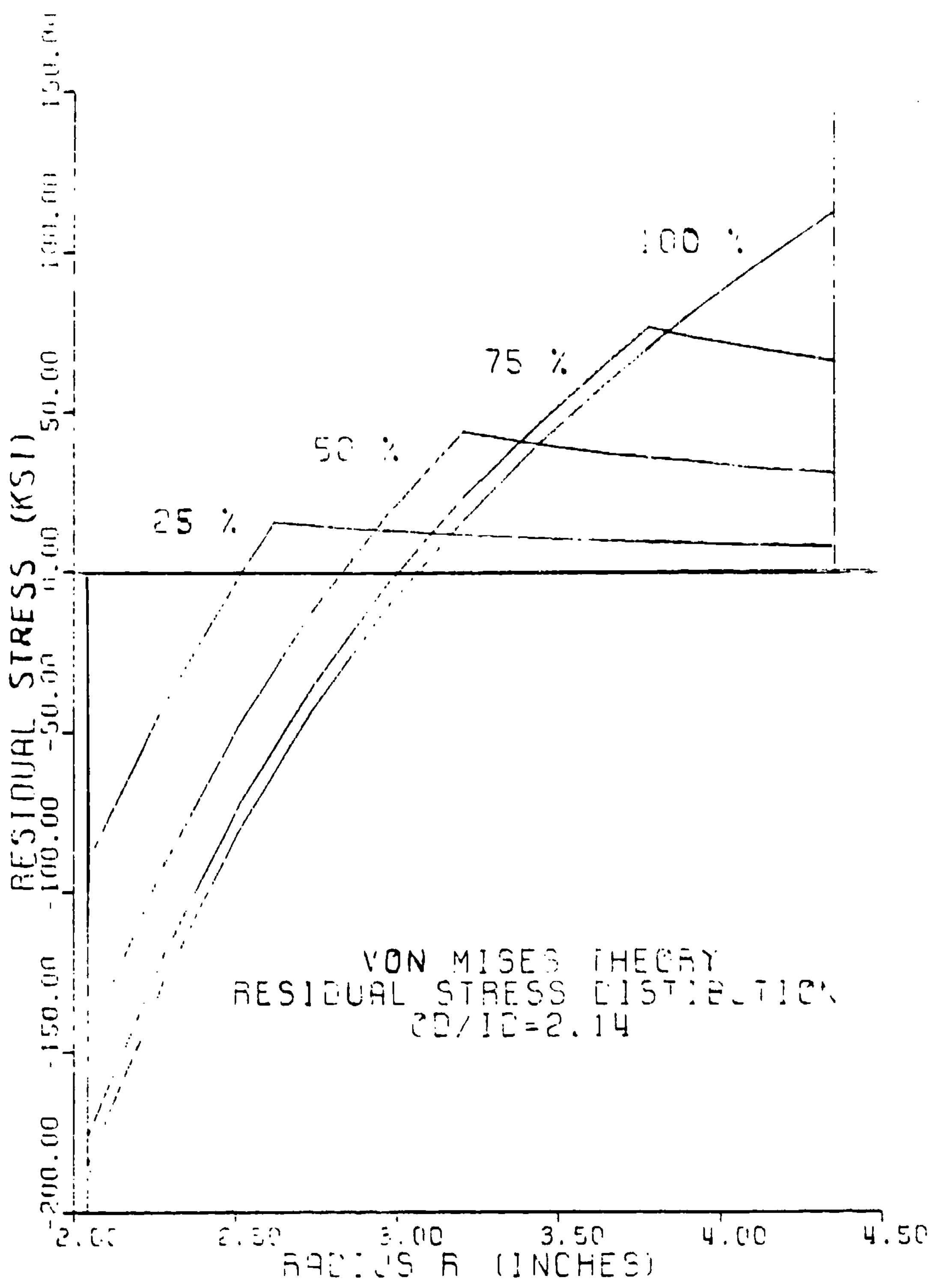

Fig. 2. Residual Stress versus Radius, OD/ID = 2.14

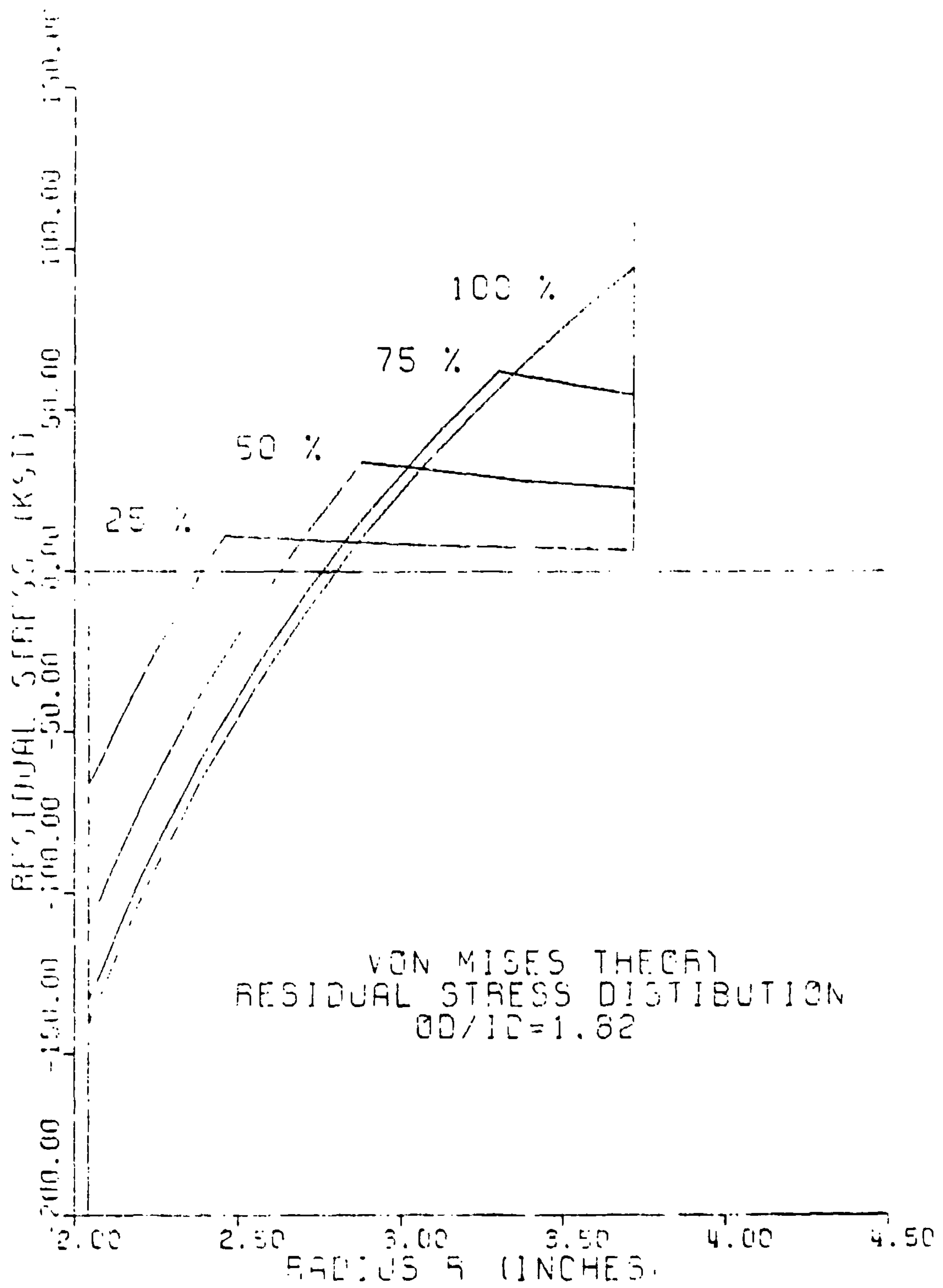

Fig. 3. Residual Stress versus Radius, OD/ID = 1.82

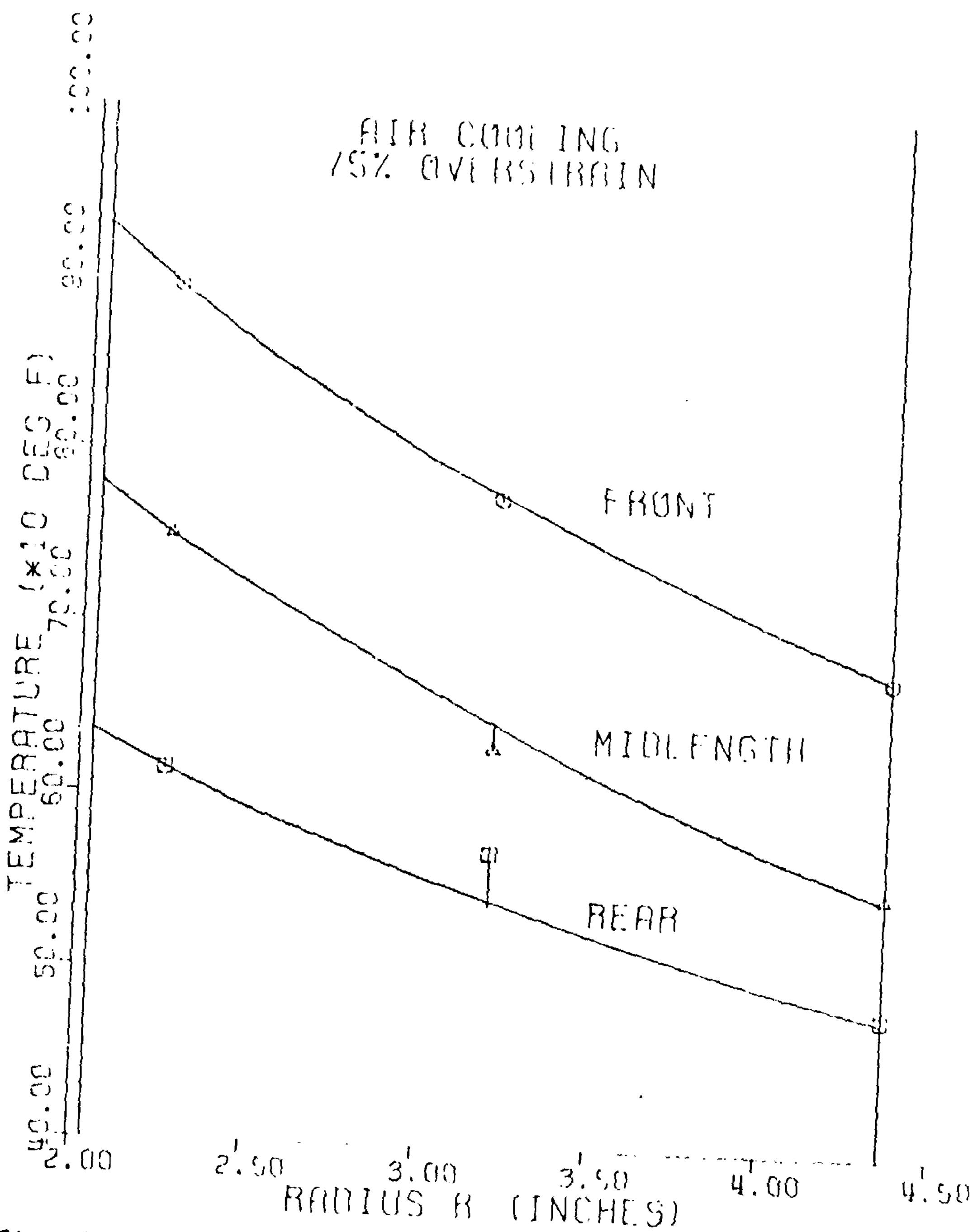

Fig. 4. Temperature Distribution, OD/ID = 2.14, for the forced air cooling condition.

Figure 5 shows the measured bore closure and its dependence upon the temperature difference ΔT between the ID and OD for the three bore temperatures which were measured at the front hot end, the mid-length and the rear exit end of the cylinders. The data points are plotted at increasing ΔT values corresponding to the progressively increasing cooling of natural convection, forced convection, air-water spray, and water spray. The curves may be approximated by an equation of the form $y = A(1-e^{B(\Delta T)})$. For example, with a bore temperature of 730°F the approximation is expressed by $BC = 0.006(1-e^{-.0165(5/9\Delta T)})$, where BC is bore closure in inches and ΔT is in degrees Farenheit.

It is apparent that the bore closure rises rapidly with small increase in ΔT but approaches a limit asymptotically as ΔT is increased beyond 200°F. This graph is for 100% overstrained cylinders of the 2.14 diameter ratio. In this case the limit is 0.006 inch for the bore temperature of 730°F. For the 950°F bore temperature the limit is more than twice as big.

Figure 6 shows a similar dependence of bore closure on ΔT for the 75% overstrained cylinders of 2.14 diameter ratio. This data did not show the well defined asymptotic nature seen in Figure 5. Also, the bore closure corresponding to any ΔT is much smaller, by a factor of about one-half at ΔT of 200°F for instance, than those for 100% overstrain.

Figure 7 shows bore closure versus ΔT for the 50% overstrained cylinders of 2.14 diameter ratio. These measured bore closures are not much different from those in the 75% overstrained cylinders. Thus, reduction from 75% to 50% overstrain does not significantly reduce the bore closure for this diameter ratio.

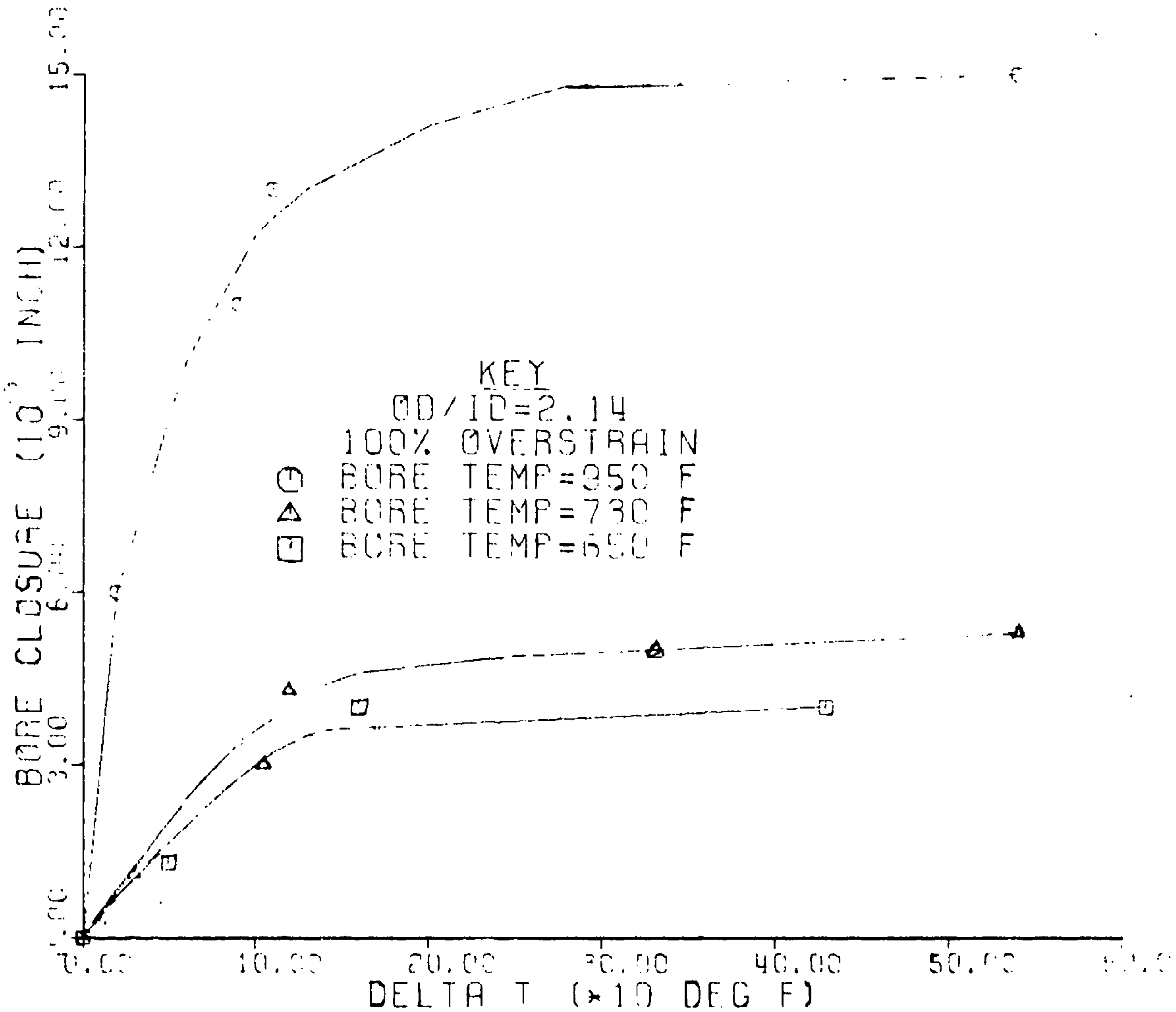

Fig. 5. Bore Closure versus Delta T, 100% Overstrain, OD/ID = 2.14

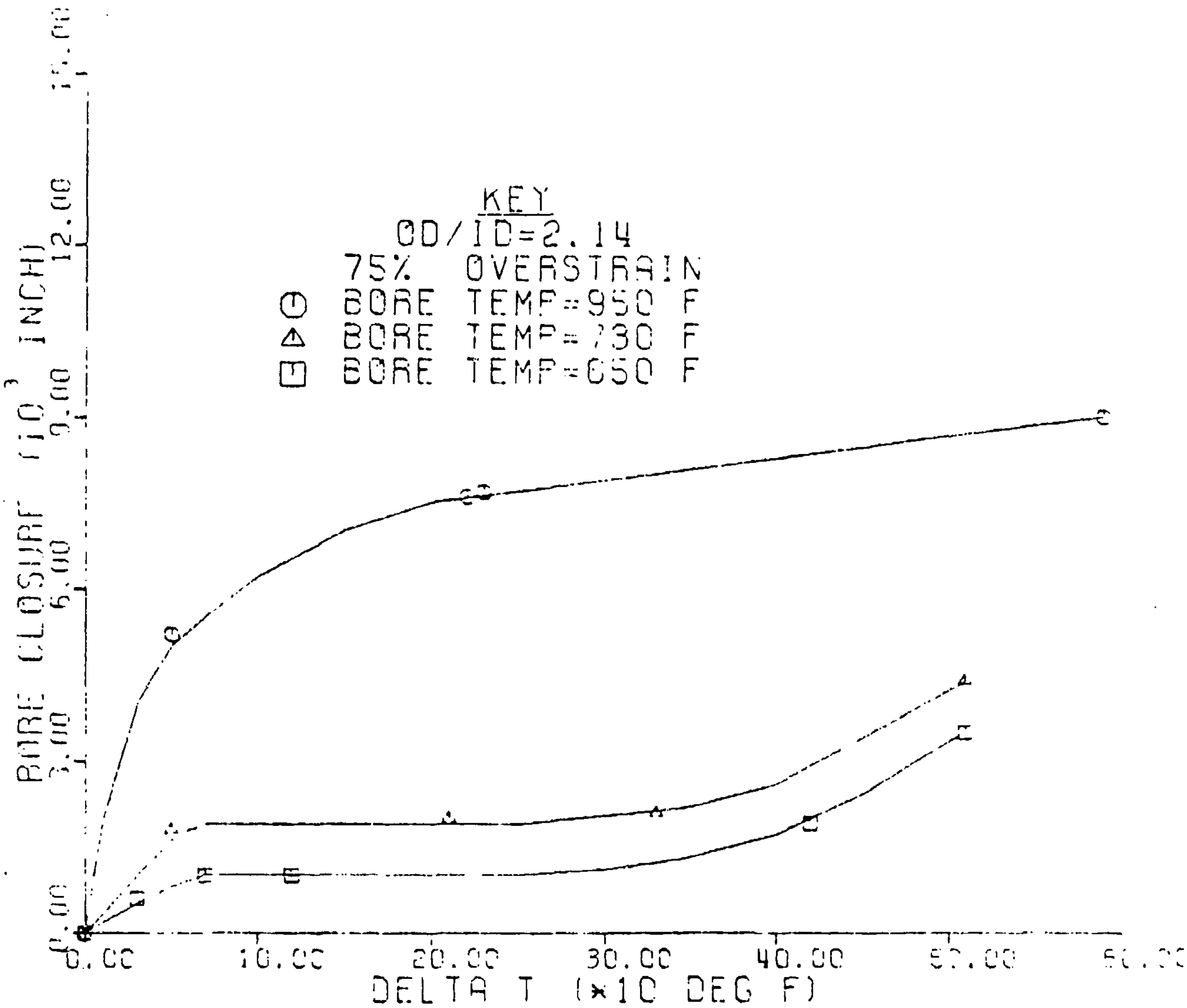

Fig. 6. Bore Closure versus Delta T, 75% Overstrain, OD/ID = 2.14

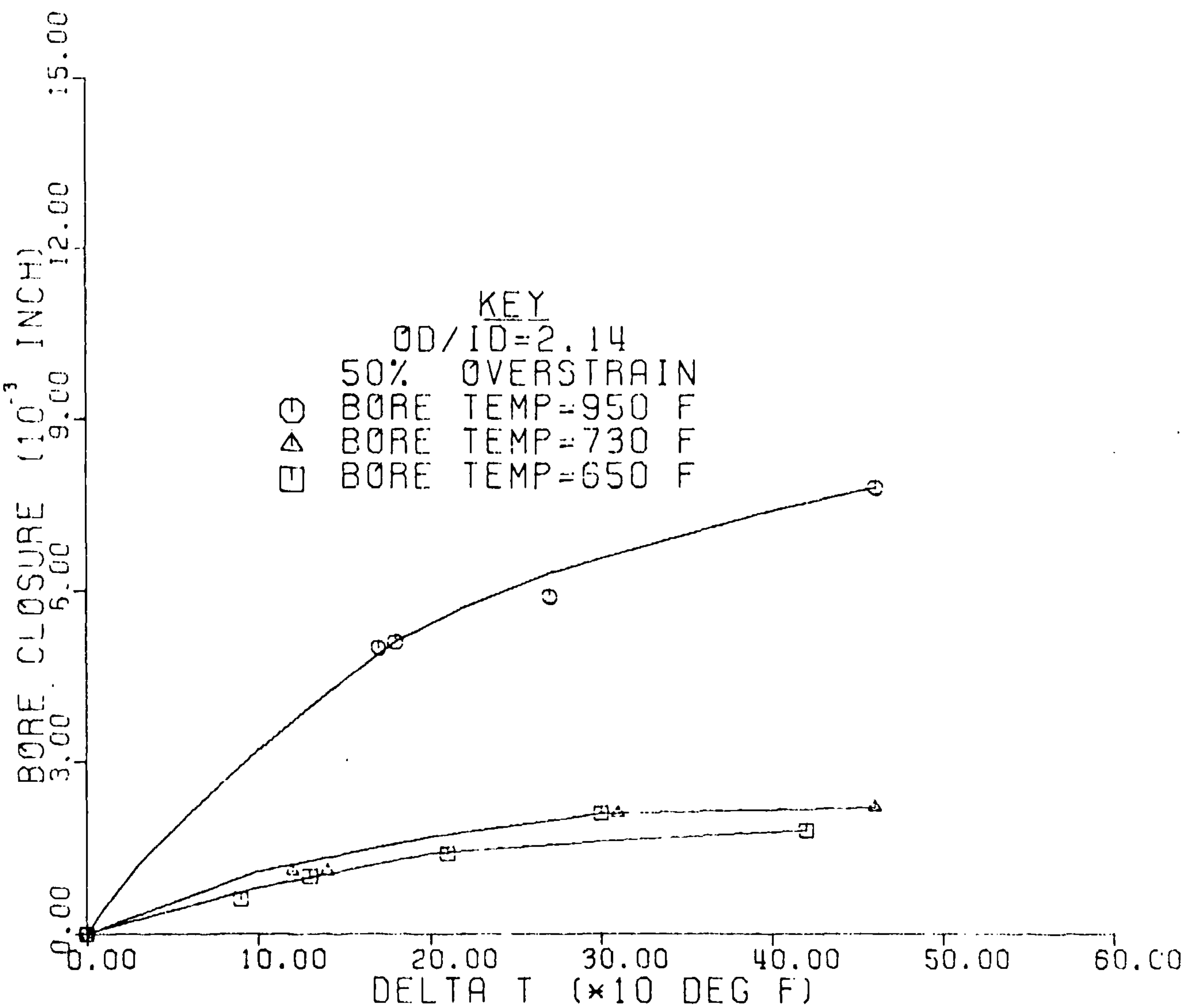

Fig. 7. Bore Closure versus Delta T, 50% Overstrain, OD/ID = 2.14

Figure 8 is a graph of the bore closure dependence on ΔT for 100% overstrained cylinders of the 1.82 diameter ratio, plotted for the hot end, the mid-length and the exit end bore temperatures. For this diameter ratio the maximum bore closures measured at ΔT near 600°F, corresponding to water cooling, are about 0.006 inch, while those at the lower bore temperatures are much less than that. Thus, the bore closures in the 1.82 diameter ratio cylinders are less than half as large as those in the 2.14 diameter ratio cylinders.

Figure 9 shows similar results for the 75% overstrained cylinders of 1.82 diameter ratio. For bore temperatures less than 730°F the bore closure is very small.

Figure 10 shows similar results for the 50% overstrained cylinders of 1.82 diameter ratio. The maximum bore closure was only about 0.003 inch even at the 950°F bore temperature.

Figure 11 is a plot of bore closure versus percent overstrain for a given ΔT of 200°F in the cylinders of 2.14 diameter ratio. The large increase in bore closure for percent overstrain greater than 75% is readily apparent here for each of the three bore temperatures. This is attributed to the larger amount of yielding during heating because of the greater depth and magnitude of ID compressive residual stress and the larger OD tensile residual stress in the 100% overstrained cylinders, see again Figure 2.

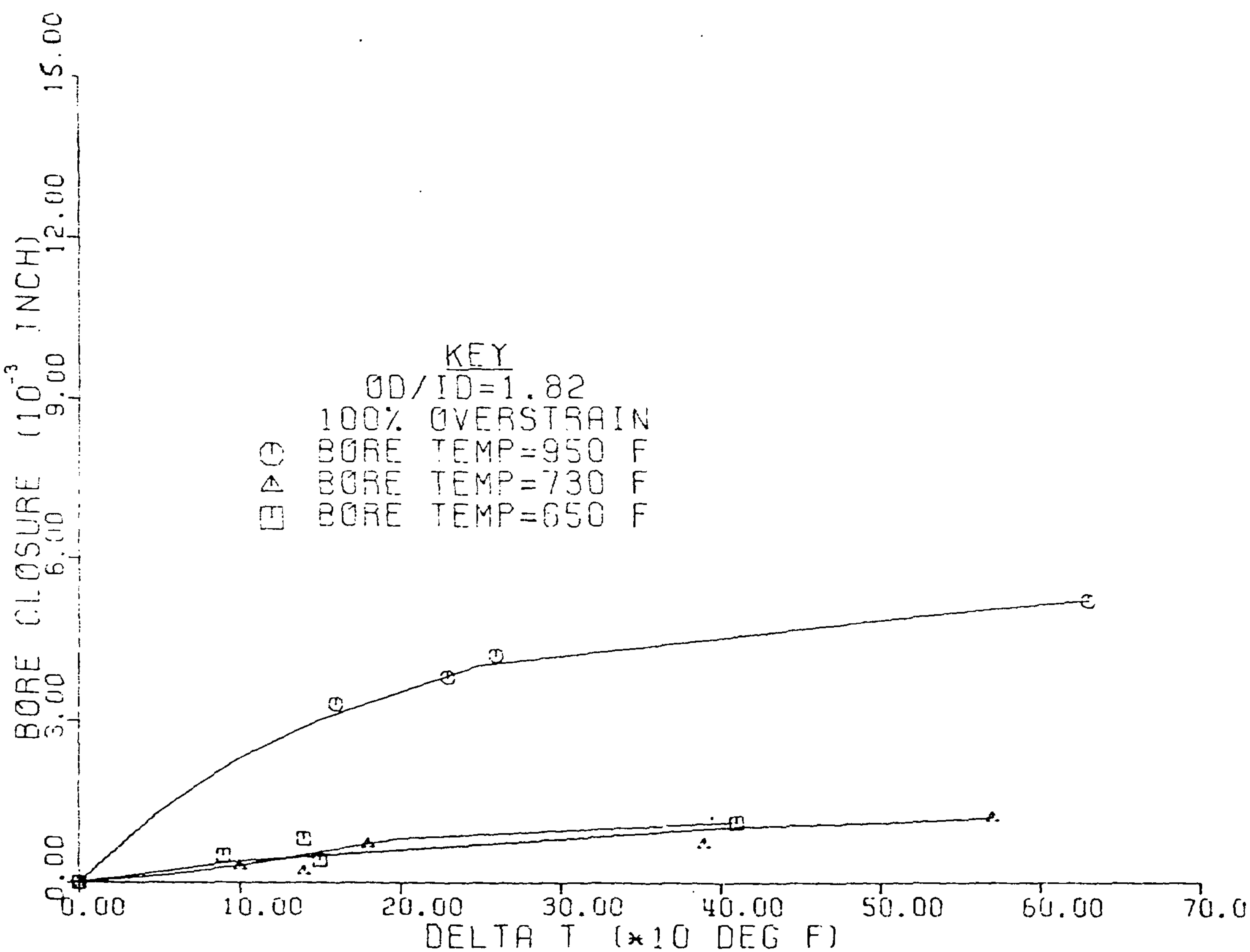

Fig. 8. Bore Closure versus Delta T, 100% Overstrain, OD/ID = 1.82

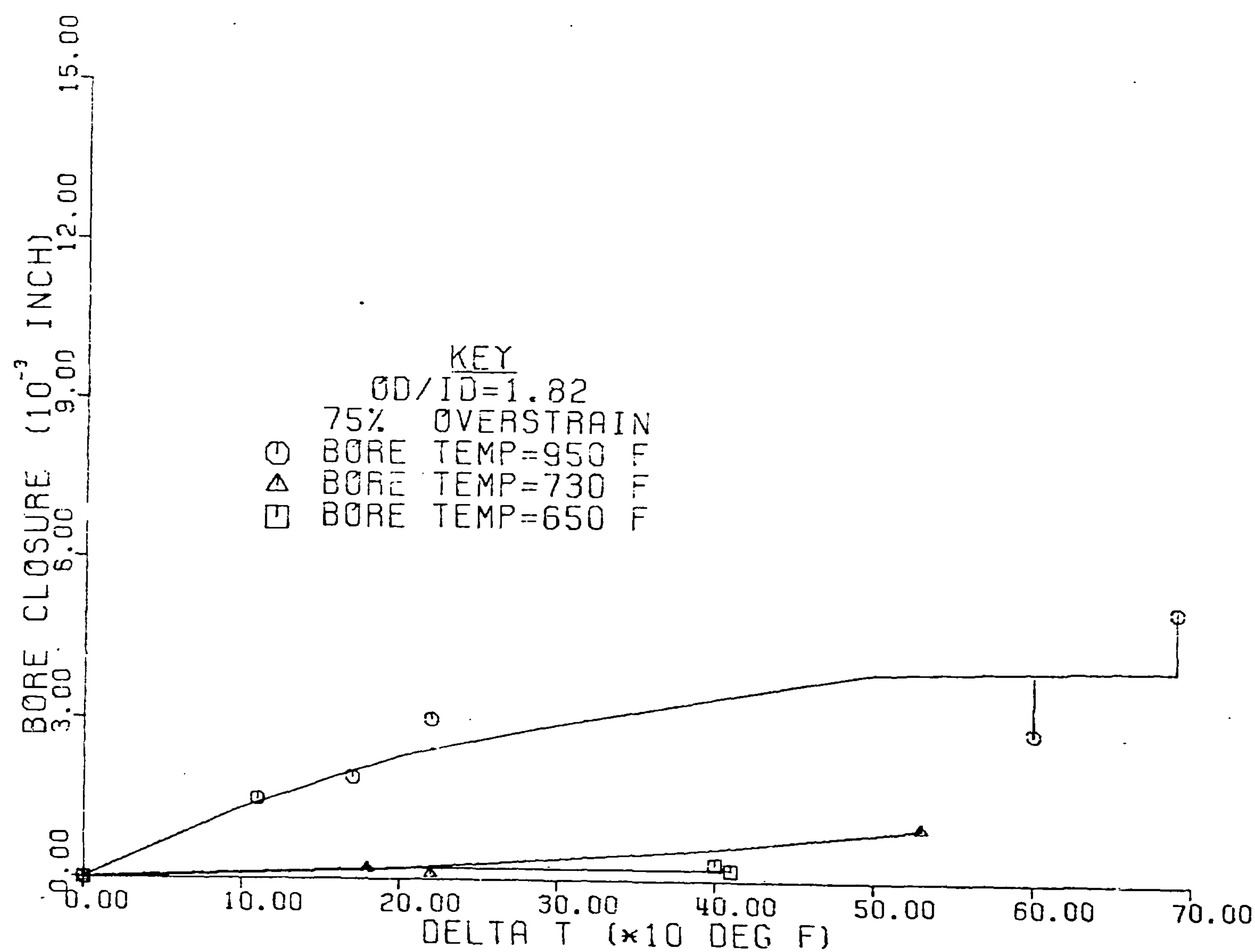

Fig. 9. Bore Closure versus Delta T, 75% Overstrain, OD/ID = 1.82

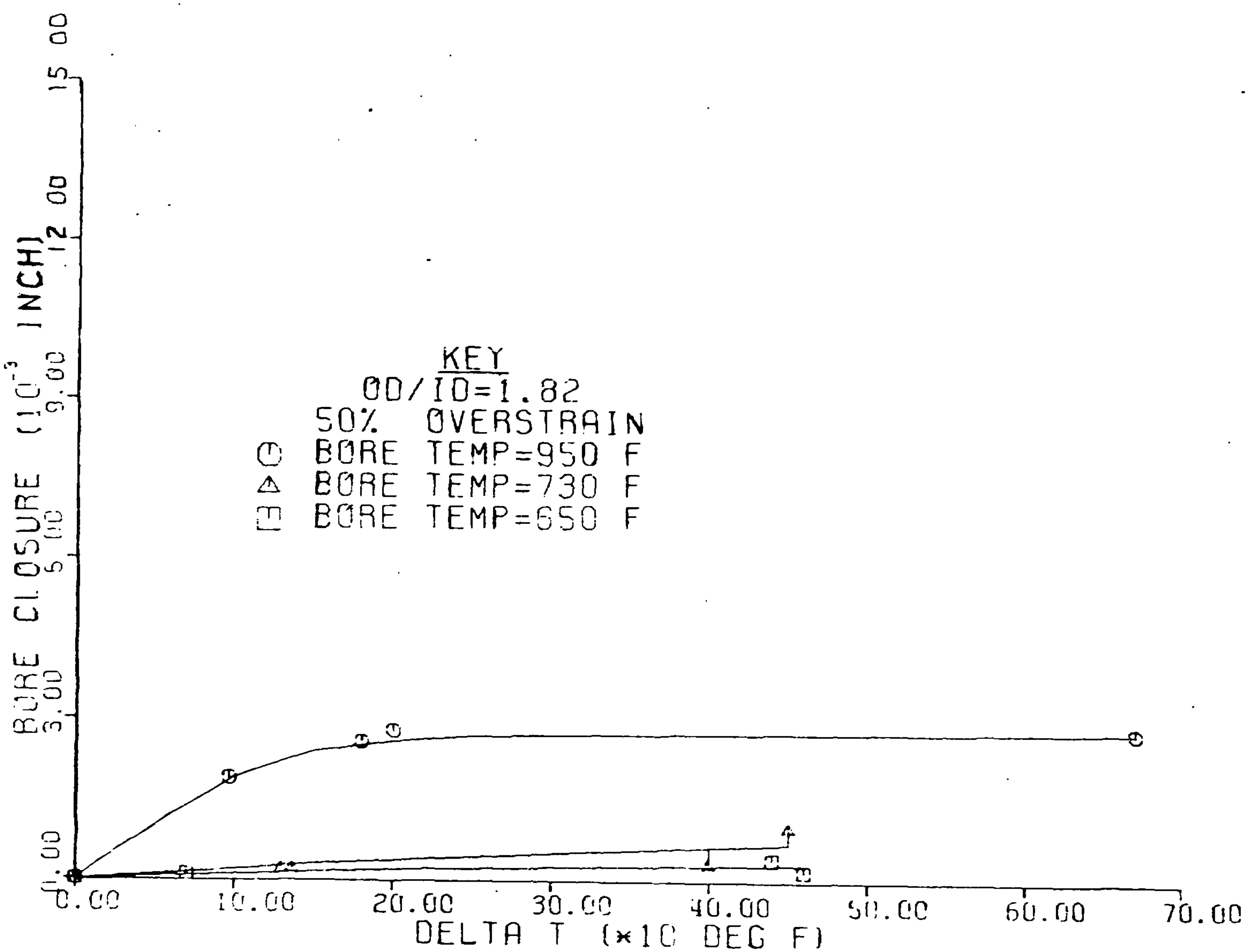

Fig. 10. Bore Closure versus Delta T, 50% Overstrain, OD/ID = 1.82

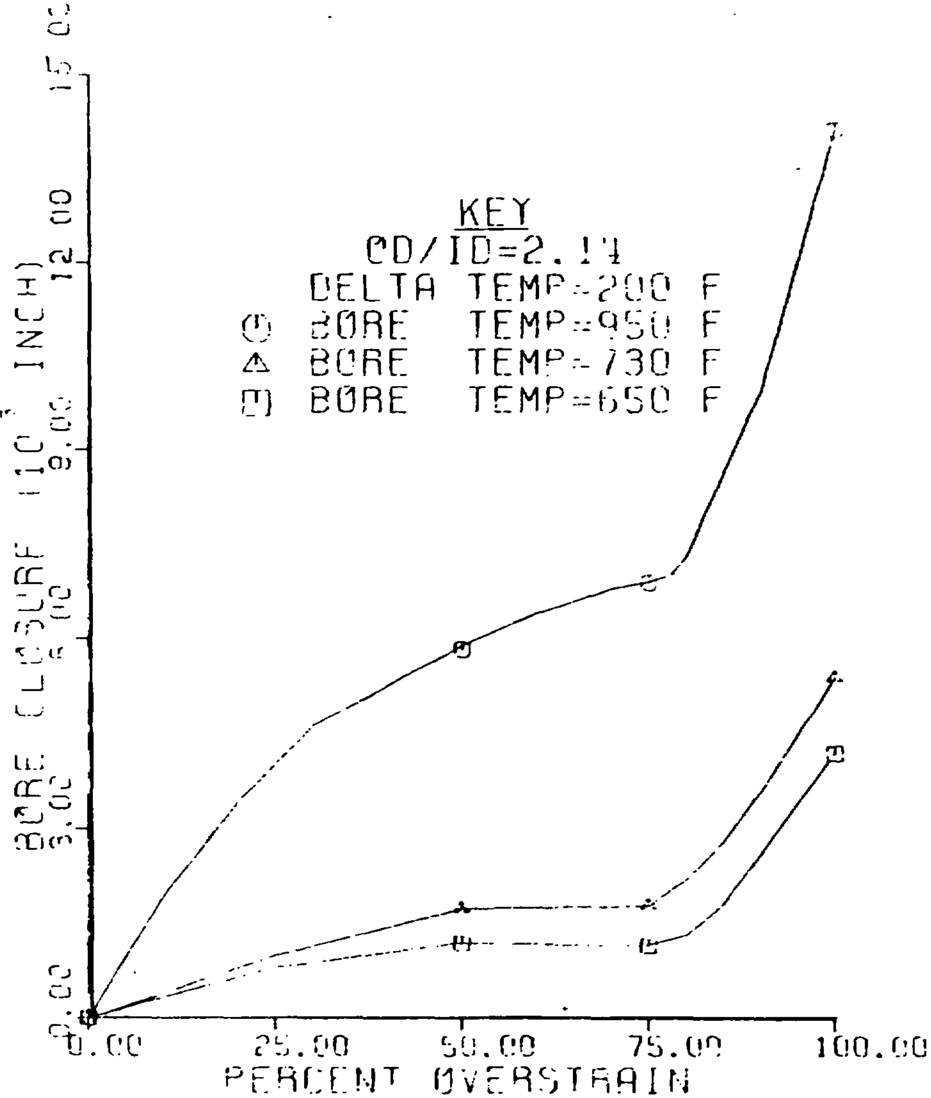

Fig. 11. Bore Closure versus Percent Overstrain for a Delta T of 200°F, OD/ID = 2.14

Figure 12 is a plot of bore closure versus percent overstrain for one-inch thick rings which were subjected to furnace heating for two hours at each of the successive temperatures from 600°F to 1000°F shown. These rings were cut from cylinders of 2.14 diameter ratio after autofrettage. Note that the bore closure scale on this graph is 1/5 that on Figure 11. These graphs indicate that the thermal gradient for a ΔT of 20[illegible] represented in Figure 11 causes bore closures about five times greater for the 100% overstrain and about three times greater for the 75% overstrain than did the uniform temperature from two hours of furnace heating represented in Figure 12.

The effect of such bore closures is not only to constrict the cylinder opening, but to reduce the residual stress levels by relaxation. The residual stress remaining was measured by slitting rings from the three locations in the cylinders.

Figure 13 is a graph of the ring separation angle ratio plotted versus percent overstrain. The ratio is formed by dividing the separation angle measured after slitting a ring of the partially overstrained specimen by the theoretical angle for 100% overstrain. From Equations (1), (3), and (4) the theoretical angle is found to be expressed in degrees by:

$$\gamma_{100\%} = \frac{8\pi\sigma_y}{\sqrt{3}\,E}\left(\frac{360}{2\pi}\right)$$

and is theoretically independent of the diameter ratio OD/ID of the ring. Here σ_y is 170,000 psi and E is 30×10^6 psi, hence $\gamma_{100\%} = 4.710$ degrees.

The upper data points were obtained from the separation angles of rings of 1.82 diameter ratio after slitting. The lower data points were obtained similarly from slitting rings of the 2.14 diameter ratio, and the single data

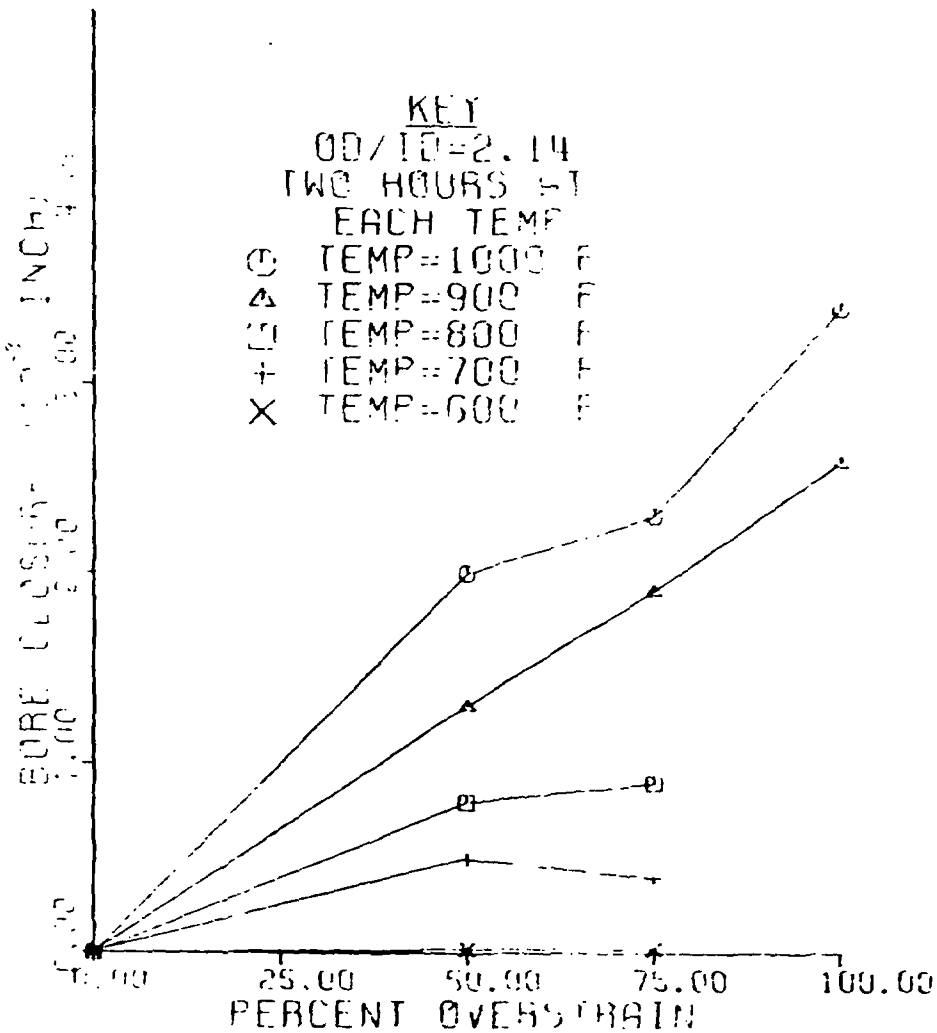

Fig. 12. Bore Closure versus Percent Overstrain for Furnace Heating, OD/ID = 2.14

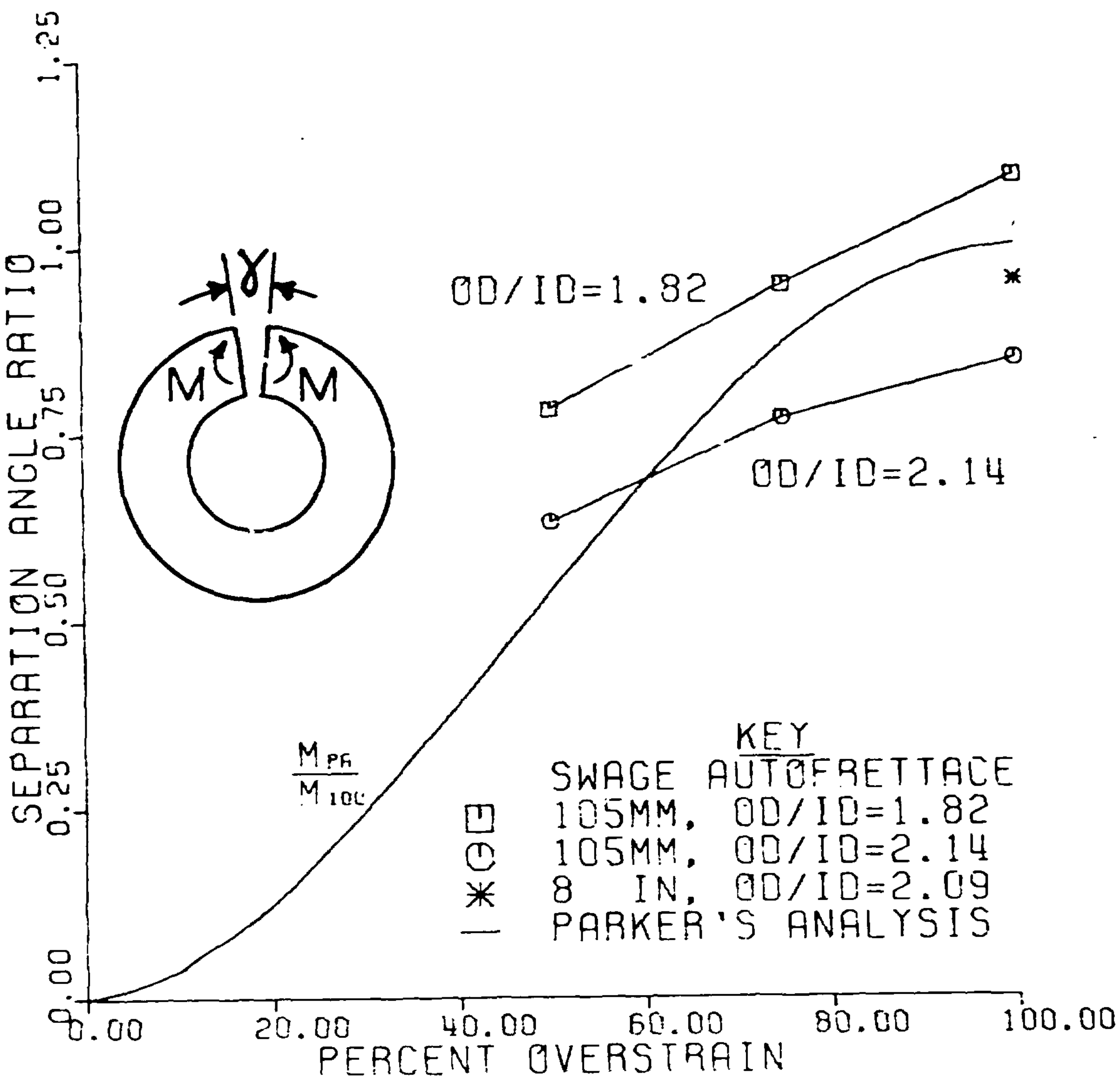

Fig. 13. Separation Angle Ratio versus Percent Overstrain for the initial autofrettaged condition, with three diameter ratios and Parker's analysis.

point from a 100% overstrained eight inch tube was from a ring of 2.09 diameter ratio. These are compared with a curve from an analysis by A. P. Parker[5] which expresses the ratio of the moments, M_{PA} for partial overstrain and M_{100} for 100% overstrain, required to close the angular gap resulting from slitting rings of 2.00 diameter ratio. The analytical curves for all other diameter ratios discussed here should be within 1% of that shown in Figure 13. The ratio of the separation angles predicted by analysis should be the same as the ratio of the moments.

Comparison of the experimental results with the curve for 2.00 diameter ratio indicates that there is a reduction of angle as the diameter ratio increases from 1.82 to 2.14. It is believed that non-ideal Bauschinger effects of reverse yielding occurring during the autofrettage process account for the discrepancies between the data and the analytical curve. Greater tensile yielding and more reversed yielding would occur at the bore of the larger diameter ratio cylinders during autofrettage, resulting in less than expected residual stress. The discrepancy from the theory is greatest at 100% overstrain, which is logical because the biggest Bauschinger effect should accompany the largest overstrain. This discrepancy at 100% overstrain is even more pronounced in the graphs of residual stress obtained from strain gage data which are shown in Figures 14 and 15.

---

[5]Parker, A. P., Underwood, J. H., Throop, J. F., and Andrasic, J. P., "Stress Intensity and Fatigue Crack Growth in a Pressurized Autofrettaged Thick Cylinder," presented in the ASTM 14th National Symposium on Fracture Mechanics on June 30, 1981, UCLA, Los Angeles, Ca.

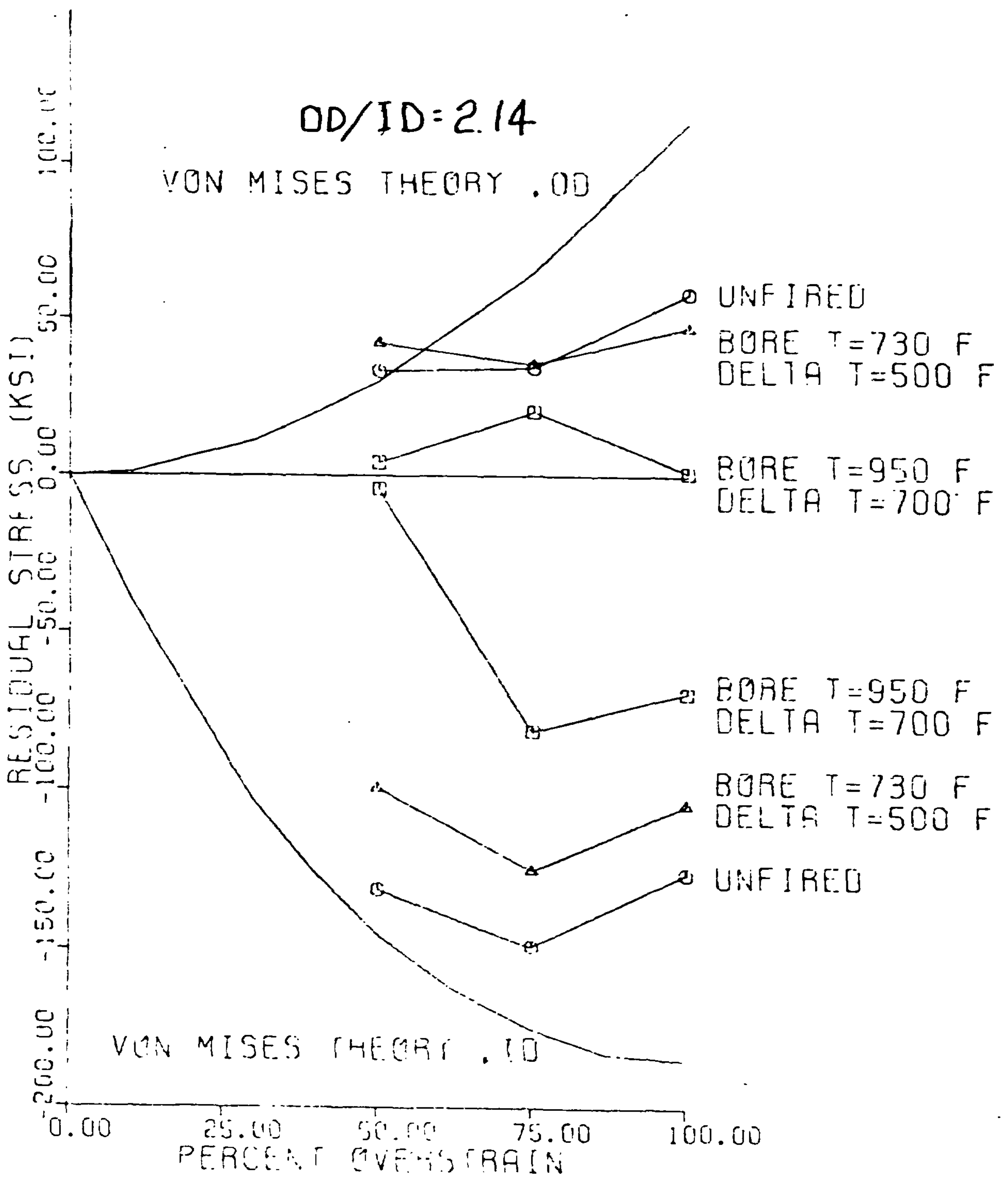

Fig. 14. Residual Stress versus Percent Overstrain for the Thermal Test Conditions, OD/ID = 2.14

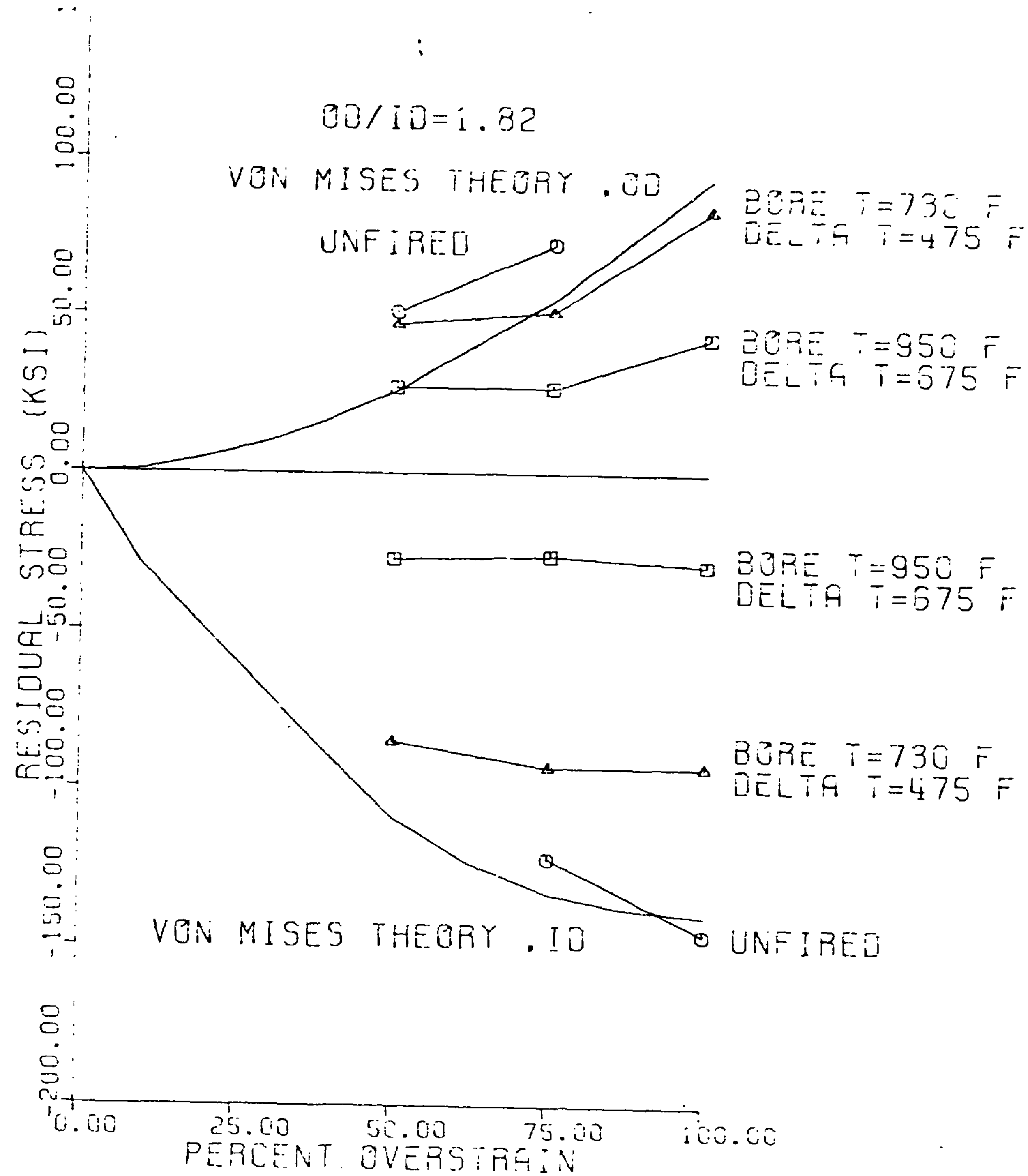

Fig. 15. Residual Stress versus Percent Overstrain for the Thermal Test Conditions, OD/ID = 1.82

Figure 14 shows the theoretical variation of tensile residual OD stress in the upper portion and that of the compressive residual bore stress in the lower portion, plotted versus percent overstrain for cylinders of 2.14 diameter ratio. Experimental measurements of residual stress relieved at strain gages next to the sawcuts when the rings were slit are also plotted for the unfired as-autofrettaged cylinders and for the thermally treated autofrettaged cylinders. At 100% overstrain the plot shows a large difference between the theory and the unfired data, in both the ID and OD residual stresses. The differences from theory are much greater than for the 75% and 50% overstrained cylinders. This is attributed to greater losses in the 100% overstrained cylinders caused by the Bauschinger effect during the autofrettage process.

It is also significant that at the elevated bore temperatures of 730°F and 950°F and the ΔT corresponding to water cooling, large losses in residual stress occurred in the 15 minute thermal exposure.

Figure 15 shows a similar graph of residual stress versus percent overstrain for the 1.82 diameter ratio cylinders. Here there is no great difference between the strain-gage measured residual stresses in the unfired autofrettaged cylinders and the theory. However, the losses of residual stress at the elevated bore temperatures and ΔT corresponding to water cooling are just as severe as in the 2.14 diameter ratio cylinders. They indicate that even for this smaller diameter ratio, water cooling of the hot cylinders can cause large loss of autofrettage residual stresses in a few minutes.

Figure 16 shows the residual bore stress ratio expressed by the ratio (σ_θ experimental)/(σ_θ theoretical) for the 2.14 diameter ratio cylinders plotted versus the bore enlargement ratio expressed by the ratio (final bore enlargement)/initial bore enlargement for each percentage overstrain.

The results from the unfired cylinders plot at the bore enlargement ratio of 1.00 and show about 30% loss from the theoretical residual bore stress in the 100% overstrained cylinders, about 15% loss in the 75% overstrained cylinders and about 10% loss in the 50% overstrained cylinder.

At the elevated bore temperatures and ΔT corresponding to water cooling the loss in residual bore stress is even greater, and is greatest in the 100% overstrained cylinders. Note that data points for some test conditions are missing in Figure 16 due to experimental problems.

Information such as in Figure 16 may provide a useful measure of thermal damage to autofrettaged cylinders, permitting one to estimate how much of the autofrettage residual bore stress remains in a cylinder after thermal treatment or after prolonged firing and cooling in service. From measured bore diameters before and after autofrettage and after thermal exposure one can determine the bore enlargement ratio and from that estimate the ratio of remaining residual stress to the theoretical autofrettage residual stress.

Figure 17 shows a similar graph of residual bore stress ratio versus bore enlargement ratio for the cylinders of 1.82 diameter ratio. The results for the unfired cylinders show very small loss in residual bore stress compared to the theoretical expected values, as mentioned earlier in regard to Figure 15. On the other hand, at the elevated bore temperatures and ΔT corresponding to

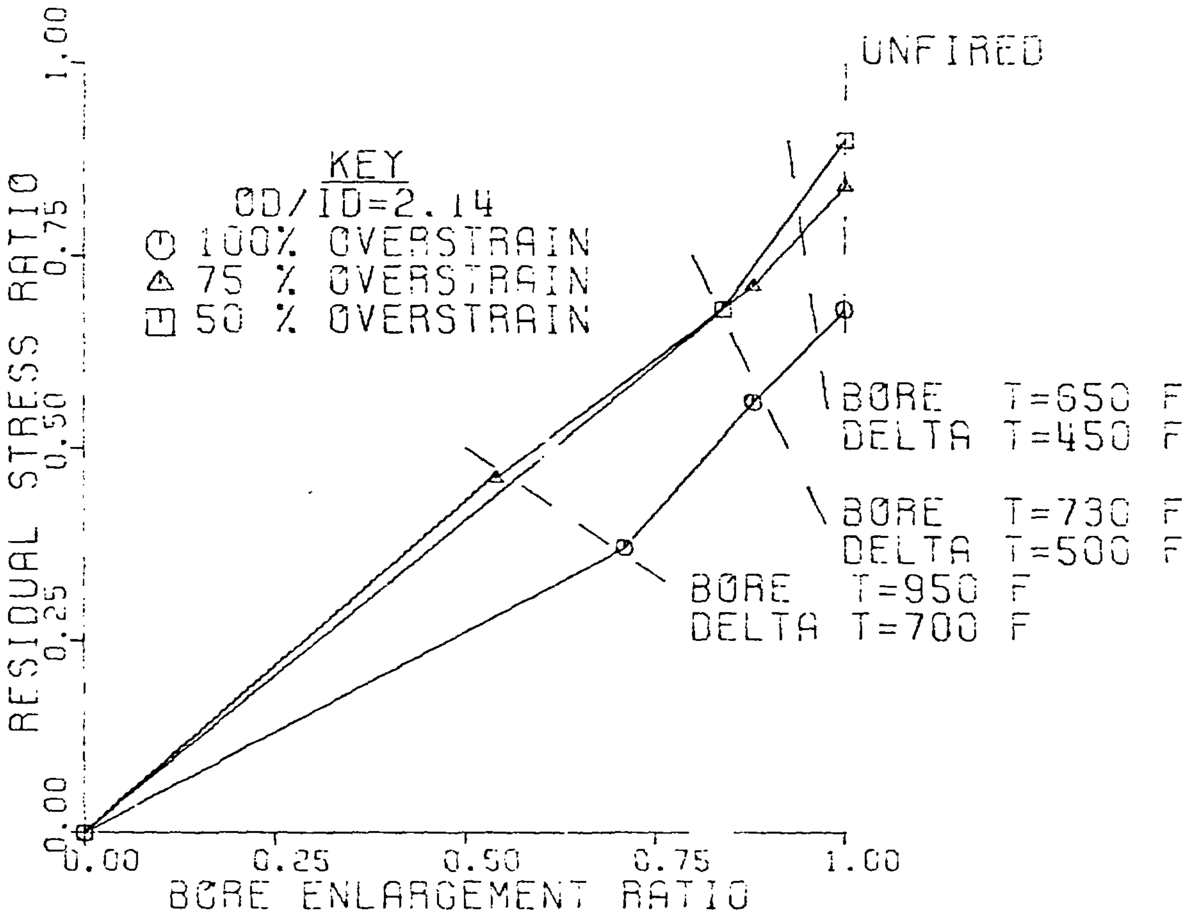

Fig. 16. Residual Stress Ratio versus Bore Enlargement Ratio for the Thermal Test Conditions, OD/ID = 2.14

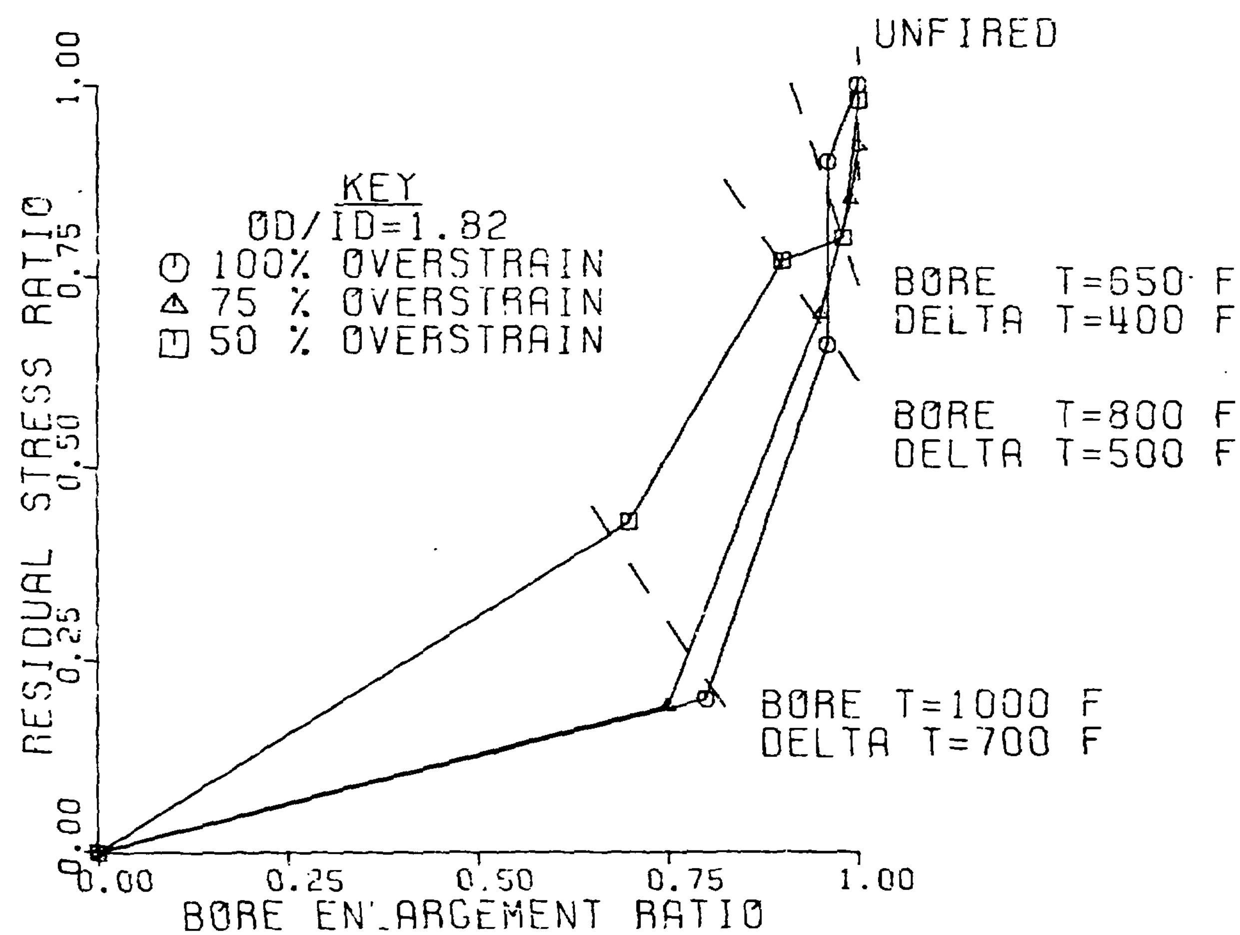

Fig. 17. Residual Stress Ratio versus Bore Enlargement Ratio for the Thermal Test Conditions, OD/ID = 1.82

water cooling a 25% decrease in bore enlargement ratio from 1.00 to 0.75 is accompanied by an 80% drop in the residual bore stress ratio, not only for the 100% overstrained cylinders but also for the 75% overstrained ones. This indicates that for the thinner wall cylinders water cooling of tubes from bore temperatures near 1000°F may practically eliminate the autofrettage residual bore stresses. At the 650°F bore temperature, however, the loss of residual bore stress is only about 20% for a decrease of about 10% in the bore enlargement ratio resulting from water cooling.

CONCLUSIONS

1. In the presence of high thermal gradients, residual stress relaxation and bore closure can occur in large diameter ratio cylinders with overstrain as low as 50%.

2. The magnitude of relaxation is significantly greater in the presence of thermal gradients as compared to uniform heating. This indicates that the primary mechanism is reverse yielding due to the combined compressive autofrettage residual and thermal stresses near the bore.

3. The magnitude of relaxation increases with increased overstrain even though there is little difference in actual compressive residual bore stress between 75% overstrain and 100% overstrain.

4. The amount of bore closure increases with measured overstrain, thermal gradient and bore temperature. The magnitude of residual bore stress relaxation is a function of the initial residual stress level and is not directly related to percent overstrain in cylinders of large diameter ratios.

REFERENCES

1. Dawson, V. C. D. and Jackson, J. W., "Investigation of the Relaxation of Residual Stresses in Autofrettaged Cylinders," Trans. of ASME, Jour. of Basic Engineering, Vol. 91, Series D, No. 1, pp. 63-66, March 1969.
2. Davidson, T. E., Barton, C. S., Reiner, A. N., and Kendall, D. P., "Overstrain of High Strength, Open End Cylinders of Intermediate Diameter Ratio," Proc. 1st International Congress on Experimental Mechanics, pp. 335-352, Pergamon Press, Oxford, 1963.
3. Timoshenko, S. and Goodier, J. N., "Theory of Elasticity," Second Edition, McGraw Hill, NY (1951), pp. 60-69, Third Edition, McGraw HIll, NY (1970), pp. 68-80.
4. Kreith, F., "Principles of Heat Transfer," International Textbook Co., Scranton, PA, 1958, pp. 25-29.
5. Parker, A. P., Underwood, J. H., Throop, J. F., and Andrasic, J. P., "Stress Intensity and Fatigue Crack Growth in a Pressurized Autofrettaged Thick Cylinder," presented in the ASTM 14th National Symposium on Fracture Mechanics on June 30, 1981, UCLA, Los Angeles, Ca.

TECHNICAL REPORT INTERNAL DISTRIBUTION LIST

	NO. OF COPIES
COMMANDER	1
CHIEF, DEVELOPMENT ENGINEERING BRANCH	1
ATTN: DRDAR-LCB-DA	1
-DM	1
-DP	1
-DR	1
-DS	1
-DC	1
CHIEF, ENGINEERING SUPPORT BRANCH	1
ATTN: DRDAR-LCB-SE	1
-SA	1
CHIEF, RESEARCH BRANCH	2
ATTN: DRDAR-LCB-RA	1
-RC	1
-RM	1
-RP	1
CHIEF, LWC MORTAR SYS. OFC.	1
ATTN: DRDAR-LCM	1
CHIEF, IMP. 81MM MORTAR OFC.	1
ATTN: DRDAR-LCB-I	1
TECHNICAL LIBRARY	5
ATTN: DRDAR-LCB-TL	
TECHNICAL PUBLICATIONS & EDITING UNIT	2
ATTN: DRDAR-LCB-TL	
DIRECTOR, OPERATIONS DIRECTORATE	1
DIRECTOR, PROCUREMENT DIRECTORATE	1
DIRECTOR, PRODUCT ASSURANCE DIRECTORATE	1

NOTE: PLEASE NOTIFY DIRECTOR, BENET WEAPONS LABORATORY, ATTN: DRDAR-LCB-TL, OF ANY REQUIRED CHANGES.

TECHNICAL REPORT EXTERNAL DISTRIBUTION LIST

	NO. OF COPIES
ASST SEC OF THE ARMY RESEARCH & DEVELOPMENT ATTN: DEP FOR SCI & TECH THE PENTAGON WASHINGTON, D.C. 20315	1
COMMANDER US ARMY MAT DEV & READ. COMD ATTN: DRCDE 5001 EISENHOWER AVE ALEXANDRIA, VA 22333	1
COMMANDER US ARMY ARRADCOM ATTN: DRDAR-LC	1
-LCA (PLASTICS TECH EVAL CEN)	1
-LCE	1
-LCM	1
-LCS	1
-LCW	1
-TSS (STINFO) DOVER, NJ 07801	2
COMMANDER US ARMY ARRCOM ATTN: DRSAR-LEP-L ROCK ISLAND ARSENAL ROCK ISLAND, IL 61299	1
DIRECTOR US ARMY BALLISTIC RESEARCH LABORATORY ATTN: DRDAR-TSB-S (STINFO) ABERDEEN PROVING GROUND, MD 21005	1
COMMANDER US ARMY ELECTRONICS COMD ATTN: TECH LIB FT MONMOUTH, NJ 07703	1
COMMANDER US ARMY MOBILITY EQUIP R&D COMD ATTN: TECH LIB FT BELVOIR, VA 22060	1

	NO. OF COPIES
COMMANDER US ARMY TANK-AUTMV R&D COMD ATTN: TECH LIB - DRDTA-UL	1
MAT LAB - DRDTA-RK WARREN, MICHIGAN 48090	1
COMMANDER US MILITARY ACADEMY ATTN: CHMN, MECH ENGR DEPT WEST POINT, NY 10996	1
US ARMY MISSILE COMD REDSTONE SCIENTIFIC INFO CEN ATTN: DOCUMENTS SECT, BLDG 4484 REDSTONE ARSENAL, AL 35898	2
COMMANDER REDSTONE ARSENAL ATTN: DRSMI-RRS	1
-RSM ALABAMA 35809	1
COMMANDER ROCK ISLAND ARSENAL ATTN: SARRI-ENM (MAT SCI DIV) ROCK ISLAND, IL 61202	1
COMMANDER HQ, US ARMY AVN SCH ATTN: OFC OF THE LIBRARIAN FT RUCKER, ALABAMA 36362	1
COMMANDER US ARMY FGN SCIENCE & TECH CEN ATTN: DRXST-SD 220 7TH STREET, N.E. CHARLOTTESVILLE, VA 22901	1
COMMANDER US ARMY MATERIALS & MECHANICS RESEARCH CENTER ATTN: TECH LIB - DRXMR-PL WATERTOWN, MASS 02172	2

NOTE: PLEASE NOTIFY COMMANDER, ARRADCOM, ATTN: BENET WEAPONS LABORATORY, DRDAR-LCB-TL, WATERVLIET ARSENAL, WATERVLIET, N.Y. 12189, OF ANY REQUIRED CHANGES.

TECHNICAL REPORT EXTERNAL DISTRIBUTION LIST (CONT.)

	NO. OF COPIES
COMMANDER US ARMY RESEARCH OFFICE P.O. BOX 12211 RESEARCH TRIANGLE PARK, NC 27709	1
COMMANDER US ARMY HARRY DIAMOND LAB ATTN: TECH LIB 2800 POWDER MILL ROAD ADELPHIA, MD 20783	1
DIRECTOR US ARMY INDUSTRIAL BASE ENG ACT ATTN: DRXPE-MT ROCK ISLAND, IL 61201	1
CHIEF, MATERIALS BRANCH US ARMY R&S GROUP, EUR BOX 65, FPO N.Y. 09510	1
COMMANDER NAVAL SURFACE WEAPONS CEN ATTN: CHIEF, MAT SCIENCE DIV DAHLGREN, VA 22448	1
DIRECTOR US NAVAL RESEARCH LAB ATTN: DIR, MECH DIV	1
CODE 26-27 (DOC LIB) WASHINGTON, D. C. 20375	1
NASA SCIENTIFIC & TECH INFO FAC. P. O. BOX 8757, ATTN: ACQ BR BALTIMORE/WASHINGTON INTL AIRPORT MARYLAND 21240	1
COMMANDER DEFENSE TECHNICAL INFO CENTER ATTN: DTIA-TCA CAMERON STATION ALEXANDRIA, VA 22314	12
METALS & CERAMICS INFO CEN BATTELLE COLUMBUS LAB 505 KING AVE COLUMBUS, OHIO 43201	1
MECHANICAL PROPERTIES DATA CTR BATTELLE COLUMBUS LAB 505 KING AVE COLUMBUS, OHIO 43201	1
MATERIEL SYSTEMS ANALYSIS ACTV ATTN: DRXSY-MP ABERDEEN PROVING GROUND MARYLAND 21005	1

NOTE: PLEASE NOTIFY COMMANDER, ARRADCOM, ATTN: BENET WEAPONS LABORATORY, DRDAR-LCB-TL, WATERVLIET ARSENAL, WATERVLIET, N.Y. 12189, OF ANY REQUIRED CHANGES.